

**DEVELOPMENT OF HYDROXYPROPYL CELLULOSE-Fe-  
DOPED NANO-TiO<sub>2</sub> PHOTOCATALYST:  
SYNTHESIS, CHARACTERIZATION AND ACTIVITY TEST**

**TEH CHAO MIN**

**UNIVERSITI SAINS MALAYSIA**

**2011**

**DEVELOPMENT OF HYDROXYPROPYL CELLULOSE-Fe-DOPED  
NANO-TiO<sub>2</sub> PHOTOCATALYST:  
SYNTHESIS, CHARACTERIZATION AND ACTIVITY TEST**

**by**

**TEH CHAO MIN**

**Thesis submitted in fulfillment of the  
requirements for the degree of  
Master of Science**

**May 2011**

## ACKNOWLEDGEMENTS

I am deeply grateful and sincerely thank my principal supervisor, Prof. Abdul Rahman Bin Mohamed for his professional guidance, kind support, encouragement and caring throughout my study. I am also especially grateful to his valuable knowledge inputs and never being tired of reading my work.

I sincerely thank all the respective staffs and technicians of School of Chemical Engineering for their help. My special thanks to Pn. Aniza, Pn. Normie Hana, Cik. Nor Ain, En. Roqib, En. Mohd Faiza, Pn. Latifah, Pn. Nor Zalilah and En. Shamsul Hidayat for their assistance throughout my study. Thanks also go to technicians from School of Material and Mineral Resources Engineering and School of Biological Science for their help with sample analyses. I would also like to express my sincere gratitude to my friends Wong Chung Leng, Tan Yong Nian and Seah Choon Ming as well as Seniors Lam Sze Mun, Sin Jin Chung and Nor Fauziah for their advice, help and support throughout my study.

I gratefully acknowledge financial support by the Universiti Sains Malaysia (USM) in the form of Research University Grant (1001/227/PJKIMIA/811068), Postgraduate Research Grant Scheme (1001/PJKIMIA/8033024) and Fellowship USM 02/09.

Last but not least, I would like to convey my gratitude to my family for their unconditional love and support.

## TABLE OF CONTENTS

	<b>PAGE</b>
<b>ACKNOWLEDGEMENTS</b>	ii
<b>TABLE OF CONTENTS</b>	iii
<b>LIST OF TABLES</b>	viii
<b>LIST OF FIGURES</b>	ix
<b>LIST OF ABBREVIATIONS</b>	xii
<b>LIST OF SYMBOLS</b>	xiv
<b>ABSTRAK</b>	xv
<b>ABSTRACT</b>	xvii
<b>CHAPTER 1: INTRODUCTION</b>	
1.1 Overview of water contaminations	1
1.2 Problem statement	3
1.3 Research objectives	5
1.4 Scope study	5
1.5 Organizations of thesis	6
<b>CHAPTER 2: LITERATURE REVIEW</b>	
2.1 Phenolic compounds	8
2.2 Decomposition of organic pollutants in wastewater by photocatalytic reactions	11
2.3 Semiconductor photocatalyst: Titanium dioxide (TiO <sub>2</sub> )	12
2.4 Mechanism of photocatalytic reaction	14
2.5 Photocatalytic degradation of phenolic compounds using TiO <sub>2</sub>	19

2.6	Surfactant	29
2.6.1	General structural features and behaviors of surfactants	29
2.6.2	Modifications of TiO <sub>2</sub> by the addition of surfactants	30
2.7	Dopants	33
2.7.1	Photocatalytic degradation of organic pollutants using single-doped TiO <sub>2</sub>	33
2.7.1.1	TiO <sub>2</sub> doped with transition metals	34
2.7.1.2	Mechanism of photocatalytic reaction using Fe-doped TiO <sub>2</sub>	37
2.8	Design of experiment (DOE)	39
2.8.1	Response surface methodology (RSM)	40
2.8.2	Box-Behnken design (BBD)	41

### **CHAPTER THREE: MATERIALS AND METHODS**

3.1	Materials and chemicals	45
3.2	Equipments	47
3.2.1	Batch reactor	47
3.3	Photocatalyst preparation	49
3.3.1	Synthesis of TiO <sub>2</sub> photocatalyst	49
3.3.2	Synthesis of Fe-doped TiO <sub>2</sub> photocatalyst	50
3.4	Characterization studies	51
3.4.1	X-ray diffraction (XRD)	51
3.4.2	Transmission electron microscopy (TEM)	51
3.4.3	Surface area and porosity measurement	52
3.4.4	UV-Vis reflection spectra analysis	52
3.5	Photocatalytic experiments	53
3.5.1	Control experiments	54

3.5.2	Effects of surfactant	55
3.5.3	Comparative study of the synthesized TiO <sub>2</sub> with commercial available TiO <sub>2</sub> (Degussa P-25)	55
3.6	Effect of operating parameters	55
3.6.1	Effect of solution pH	55
3.6.2	Effect of TiO <sub>2</sub> loading	56
3.6.3	Effect of initial phenol concentration	56
3.7	Kinetics studies	56
3.7.1	Photocatalytic degradation kinetics of phenol	56
3.7.2	Reaction order and kinetic rate constant	58
3.7.3	Langmuir-Hinshelwood model	59
3.7.4	Initial reaction rate	61
3.8	Study of metal doped TiO <sub>2</sub> using response surface methodology (RSM)	62
3.8.1	Design of experiment (DOE)	62
3.8.2	Model optimization and validation	66
3.9	Performance of HPC-modified-Fe-doped TiO <sub>2</sub> under solar irradiation	66
3.10	Sample analysis	67
3.10.1	High performance liquid chromatography (HPLC)	67
3.10.2	Total organic carbon (TOC)	67

## **CHAPTER 4: RESULTS AND DISCUSSION**

4.1	Effects of surfactant	69
4.1.1	Photocatalyst characterization	69
4.1.1.1	X-ray diffraction (XRD)	69
4.1.1.2	Transmission electron microscopy (TEM)	73

	4.1.1.3	Surface area and porosity measurement	75
4.1.2		Photocatalytic performance	77
	4.1.2.1	Control experiments	77
	4.1.2.2	Effects of hydroxypropyl cellulose (HPC) concentration	80
	4.1.2.3	Comparative study of the synthesized TiO <sub>2</sub> with commercial available TiO <sub>2</sub> (Degussa P-25)	83
	4.1.2.4	Process parameters studies	84
		4.1.2.4 (a) Effect of solution pH	84
		4.1.2.4 (b) Effect of TiO <sub>2</sub> loading	87
		4.1.2.4 (c) Effect of initial phenol concentration	90
4.2		Kinetic studies	92
	4.2.1	Reaction order and kinetic rate constant	92
	4.2.2	Initial reaction rate	94
4.3		Effects of dopant	96
	4.3.1	Characterization of HPC-modified-Fe-doped TiO <sub>2</sub>	96
		4.3.1.1 X-ray diffraction (XRD)	96
		4.3.1.2 UV-Vis reflection spectra analysis	99
	4.3.2	Photocatalytic activity study of HPC-modified-Fe-doped TiO <sub>2</sub> photocatalyst using RSM	103
		4.3.2.1 Model fitting	103
		4.3.2.2 Regression analysis	105
		4.3.2.3 Response surface plot	107
		4.3.2.4 Model optimization and validation	110
	4.3.3	Performance of HPC-modified-Fe-doped TiO <sub>2</sub> under solar irradiation	111
4.4		Mineralization studies of phenol using HPC-modified-Fe-doped TiO <sub>2</sub>	113

## **CHAPTER 5: CONCLUSIONS AND RECOMMENDATIONS**

5.1 Conclusions 115

5.2 Recommendations 117

**REFERENCES** 119

**LIST OF PUBLICATIONS** 131



## LIST OF TABLES

		<b>Page</b>
Table 2.1	Summary of studies on photocatalytic degradation of phenolic compounds in wastewater in the presence of TiO <sub>2</sub> as photocatalyst	21
Table 2.2	Optimum dopant concentration used by researchers to improve the efficiency of catalyst	36
Table 2.3	Example of Box-Behnken Design for a three factors study* (Mason <i>et al.</i> , 2003)	40
Table 3.1	List of materials and chemicals	46
Table 3.2	Experimental range and levels of independent variables for Fe-doped TiO <sub>2</sub>	64
Table 3.3	Design matrix for experimental factors for Fe-doped TiO <sub>2</sub>	65
Table 4.1	Structure parameters of TiO <sub>2</sub> with different concentrations of HPC	72
Table 4.2	The values of apparent kinetics rate constant (k <sub>app</sub> ) and correlation coefficient (R <sup>2</sup> ) at different initial phenol concentrations.	94
Table 4.3	Structure parameters of TiO <sub>2</sub> with different concentrations of Fe <sup>3+</sup>	98
Table 4.4	Band gap energy and band edge wavelength of Fe-doped TiO <sub>2</sub> different Fe <sup>3+</sup> concentrations	101
Table 4.5	Experimental design matrix and results for Fe-doped TiO <sub>2</sub>	104
Table 4.6	ANOVA for model regression of Fe-doped TiO <sub>2</sub>	106
Table 4.7	Design Expert predicted and experimental results	111
Table 4.8	Percentage of phenol degraded measured by HPLC and TOC removal under irradiation of UV light (λ = 365nm) and direct solar irradiation	113

## LIST OF FIGURES

		<b>Page</b>
Figure 2.1	Positions of band edges of some semiconductors in contact with aqueous electrolyte (Schiavello, 1997).	14
Figure 2.2	Processes of photocatalysis at semiconductor particles. The numbers represent to the mechanistic steps in the text. Paths 2 and 5 which increase with decreasing crystallite size of the particle are shown by “increase” (M. Kaneko and Okura, 2002).	17
Figure 2.3	Simplified reaction mechanism of phenol degradation (Okamoto et al., 1985).	18
Figure 2.4	Overall mechanism of phenol degradation by Fe-doped TiO <sub>2</sub> under UV light and visible light (Tong et al., 2008).	39
Figure 2.5	Three factor Box-Behnken design (coded factor levels) (Mason <i>et al.</i> , 2003).	43
Figure 3.1	Schematic diagram of experimental apparatus for photocatalytic degradation of phenol.	48
Figure 3.2	Flow diagram of Fe-doped TiO <sub>2</sub> preparation procedures.	50
Figure 4.1	XRD patterns of Degussa P-25 TiO <sub>2</sub> and synthesized TiO <sub>2</sub> at different HPC concentrations.	70
Figure 4.2	TEM images of photocatalysts (a) TS(0.0), (b) TS(0.5), (c) TS(1.0) and (d) TS(1.5).	74
Figure 4.3	Comparison of phenol degradation in the dark, photolysis, adsorption and photocatalysis. (Solution pH = 6.0, $\lambda = 256\text{nm}$ ; TiO <sub>2</sub> loading = 1g/L; initial phenol concentration = 50 mg/L; air flow rate = 2.5L/min).	78
Figure 4.4	Percentage of phenol remaining plotted as a function of reaction time for TiO <sub>2</sub> loaded with different concentration of HPC under UV ( $\lambda=256\text{nm}$ ) irradiation. (Solution pH = 6.0; air flow rate = 2.5L/min; [TiO <sub>2</sub> ] = 1g/L; [phenol] = 50mg/L).	80

Figure 4.5	Effect of HPC loading on the efficiency of phenol removal under UV ( $\lambda=256\text{nm}$ ) irradiation. (Solution pH = 6.0; air flow rate = 2.5L/min; $[\text{TiO}_2] = 1\text{g/L}$ ; $[\text{phenol}] = 50\text{mg/L}$ ).	81
Figure 4.6	Comparison of photocatalytic activity between HPC loaded $\text{TiO}_2$ (1g/L) with Degussa P-25 under UV ( $\lambda=256\text{nm}$ ) irradiation. (Solution pH = 6.0; air flow rate = 2.5L/min; $[\text{TiO}_2] = 1\text{g/L}$ ; $[\text{phenol}] = 50\text{mg/L}$ ).	83
Figure 4.7	Effect of solution pH on the degradation of phenol under UV ( $\lambda=256\text{nm}$ ) irradiation. (Air flow rate = 2.5L/min; $[\text{TiO}_2] = 1\text{g/L}$ ; $[\text{phenol}] = 50\text{mg/L}$ ).	85
Figure 4.8	Effect of $\text{TiO}_2$ loading on the degradation of phenol under UV ( $\lambda=256\text{nm}$ ) irradiation. (Solution pH = 6.0; air flow rate = 2.5L/min; $[\text{phenol}] = 50\text{mg/L}$ ).	89
Figure 4.9	Effect of initial phenol concentration on the degradation of phenol under UV ( $\lambda=256\text{nm}$ ) irradiation. (Solution pH = 6.0; air flow rate = 2.5L/min; $[\text{TiO}_2] = 1\text{g/L}$ ).	90
Figure 4.10	Kinetics of phenol degradation for different phenol initial concentrations in the presence of TS (1.0). (Solution pH = 6.0; air flow rate = 2.5L/min; $[\text{TiO}_2] = 1.0\text{g/L}$ ).	93
Figure 4.11	Plot of $1/r$ against $1/C$ for phenol degradation using TS (1.0).	95
Figure 4.12	XRD patterns of HPC-modified-Fe-doped $\text{TiO}_2$ at different $\text{Fe}^{3+}$ concentrations.	96
Figure 4.13	UV-Vis reflection spectra of HPC-modified Fe-doped $\text{TiO}_2$ at different $\text{Fe}^{3+}$ concentrations.	99
Figure 4.14	Energy band gap of HPC-modified Fe-doped $\text{TiO}_2$ at different $\text{Fe}^{3+}$ concentrations.	101
Figure 4.15	Response surface plot for apparent phenol degradation rate constant as a function of phenol concentration and dopant concentration ( $\text{TiO}_2$ loading = 0.55g/L) for Fe-doped $\text{TiO}_2$ .	107
Figure 4.16	Response surface plot for apparent phenol degradation rate constant as a function of $\text{TiO}_2$ concentration and dopant concentration (phenol concentration = 50 mg/L) for Fe-doped $\text{TiO}_2$ .	109

Figure 4.17	Response surface plot for apparent phenol degradation rate constant as a function of TiO <sub>2</sub> concentration and phenol concentration (dopant concentration = 0.50 wt%) for Fe-doped TiO <sub>2</sub> .	110
Figure 4.18	Percentage of phenol remaining plotted as a function of reaction time using doped TiO <sub>2</sub> under solar irradiation (Solution pH = 6.0; air flow rate = 2.5L/min; [TiO <sub>2</sub> ] = 0.94g/L; [phenol] = 10.48mg/L).	112

## LIST OF ABBREVIATIONS

$A_{ads}$	Reactant adsorbed on the surface of photocatalyst
ANOVA	Analysis of variance
AOPs	Advanced oxidation processes
ATSDR	Agency for Toxic Substances and Disease Registry
BBD	Box-Behnken design
BET	Brunauer-Emmett-Teller
BPA	Bisphenol A
CB	Conduction band
CCD	Central composite design
CO <sub>2</sub>	Carbon dioxide
CV	Coefficient of variance
3D	Three dimensional
DEA	Diethanolamine
$DF$	Degree of freedom
DI	Deionized water
DCP	Dichlorophenol
DNP	Dinitrophenol
DOC	Dissolved oxygen concentration
DOE	Design of experiments
$e^-$	electrons
$E_{bg}$	Band gap energy
EDC	Endocrine-disrupting chemical
EHC	Environmental Health Criteria
$F$ -value	Fisher value
$FW$	Full width at half maximum of the XRD diffraction peak
$H^+$	Positive hydrogen cation
$h^+$	Positive hole
HCl	Hydrochloric acid
HNO <sub>3</sub>	Nitric acid
H <sub>2</sub> O	Water
H <sub>2</sub> O <sub>2</sub>	Hydrogen peroxide
HPC	Hydroxypropyl cellulose

HPLC	High performance liquid chromatography
IC	Inorganic carbon
<i>i</i> -PrOH	Isopropanol
IUPAC	International Union of Pure and Applied Chemistry
KHP	Potassium hydrogen phthalate
L-H	Langmuir-Hinshelwood
O <sub>2</sub>	Oxygen
Ox	Oxidation
Prob>F	Probability value greater than Fisher value
<i>product<sub>ads</sub></i>	Product adsorbed on the surface of photocatalyst
Na	Sodium
NaOH	Sodium hydroxide
NHE	Normal hydrogen electrode
NPOC	Non-purgeable organic carbon
Red	Reduction
RSM	Response surface methodology
TiO <sub>2</sub>	Titanium dioxide
TC	Total carbon
TEM	Transmission electron microscopy
TOC	Total organic carbon
TTIP	Titanium tetraisopropoxide
USEPA	United State Environmental Protection Agency
UV/Vis DRS	UV/Vis – diffuse reflectance spectroscopy
UV light	Ultra-violet light
VB	Valence band
WHO	World Health Organization
XRD	X-ray diffraction

## LIST OF SYMBOLS

Symbol	Description	Unit
$C$	Phenol concentration and time $t$	mg/L
$C_0$	Initial phenol concentration	mg/L
cb	Conduction band	-
cp	Centipoise	Kg/m.s
$dc/dt$	Differential of C polynomial with respect to $t$	-
$e^-$	Electron	-
$E_{bg}$	Bandgap energy	eV
$h^+$	Hole	-
$h\nu$	Photon energy	eV
$HO_2^\bullet$	Hyperoxyl radical	-
$K$	Adsorption equilibrium rate constant	L/mg
$k_{app}$	Pseudo-first-order rate constant	min <sup>-1</sup>
$k_{L-H}$	Reaction rate constant	mg/L.min
$O_2^{\bullet-}$	Superoxide radical anion	-
$OH^-$	Hydroxyl ion	-
$\bullet OH$	Hydroxyl radical	-
$pH_{pzc}$	Point of zero charge	-
$R$	Reflectance at a given photon energy of $h\nu$	-
$R_{max}/R_{min}$	Maximum/minimum value of reflectance	-
$R^2$	Coefficient of correlation	-
$r$	Reaction rate	mg/L.min
$t$	Time	min
T	Temperature	°C
wt%	Weight in percent	g

### Greek symbols

$\lambda$	Wavelength	nm
$\alpha$	Absorption coefficient	-
$\theta$	Surface coverage	-

**PEMBANGUNAN NANO-TiO<sub>2</sub> FOTOMANGKIN UBAHSUAI DENGAN  
HIDROKSIPROPIL SELULOSA DAN FERUM: SINTESIS, PENCIRIAN  
DAN UJIKAJI AKTIVITI**

**ABSTRAK**

Pencemaran air oleh bahan cemar organik merupakan masalah yang semakin meruncing dan telah menjadi keprihatinan global. Oleh itu, adalah amat penting untuk mendegradasikan bahan cemar organik tersebut sebelum ianya dibuang ke alam sekitar. Kebanyakan bahan cemar tidak dapat didegradasikan oleh teknik lazim seperti pengelompokan, pemendakan, penjerapan, pemisahan membran dan sebagainya. Maka, proses pengoksidaan lanjutan (AOP's) menjadi salah satu cara unggul yang telah diguna dan dipelajari secara meluas dalam proses degradasi bahan buangan industri. Fotopemangkinan heterogen yang menggunakan nano-TiO<sub>2</sub> sebagai fotomangkin telah dipelajari dalam projek ini. Nano-TiO<sub>2</sub> telah berjaya disediakan melalui cara sol-gel bermangkin asid dan fotomangkin yang disediakan tersebut telah dianalisa dengan Brunauer-Emmett-Teller (BET), belauan sinar-X (XRD), mikroskop penghantaran elektron (TEM) dan spektroskopi kepantulan UV-Vis (UV-Vis DRS). Aktiviti fotopemangkinan TiO<sub>2</sub> yang disedia telah diuji oleh fotodegradasi larutan fenol dalam reaktor kelompok. Selulosa hidroksipropil (HPC) telah ditambahkan ke dalam TiO<sub>2</sub> semasa penyediaan sol sebagai surfaktan. Penambahan HPC sebanyak 1g/L ke dalam TiO<sub>2</sub> dikenal pasti berjaya mengurangkan pengelompokan partikel-partikel dan menghasilkan TiO<sub>2</sub> dengan luas permukaan yang lebih tinggi. TiO<sub>2</sub> dengan luas permukaan tinggi ini menunjukkan aktiviti fotopemangkinan yang lebih baik berbanding dengan TiO<sub>2</sub> tanpa surfaktan dan Degussa P-25. Kesan daripada pendopan logam juga dipelajari dengan mendop TiO<sub>2</sub>



dengan  $\text{Fe}^{3+}$ . Kepekatan optimum bahan dopan  $\text{Fe}^{3+}$  telah dikenalpastikan sebagai 0.25 wt%. Metodologi respon permukaan (RSM) berdasarkan reka bentuk Box-Behnken (BBD) telah digunakan untuk menilai kesan daripada parameter operasi. Kepekatan fotomangkin = 0.94g/L, kepekatan larutan fenol = 10.48mg/L dan kepekatan  $\text{Fe}^{3+}$  = 0.25 wt% merupakan keadaan optimum untuk fotodegradasi fenol. Fotomangkin yang disediakan dalam projek didapati berjaya menguraikan 98.24% dan 85.0% fenol masing-masing di bawah penyinaran dekat UV ( $\lambda = 365\text{nm}$ ) dan penyinaran oleh cahaya matahari secara langsung.

**DEVELOPMENT OF HYDROXYPROPYL CELLULOSE-Fe-DOPED NANO-TiO<sub>2</sub> PHOTOCATALYST: SYNTHESIS, CHARACTERIZATION AND ACTIVITY TEST**

**ABSTRACT**

Water pollution by organic pollutants is an ever increasing problem for the global concerns. Therefore, it is important to degrade these pollutants completely before they are discharged to the environment. Most of the pollutants cannot be effectively degraded by conventional techniques such as flocculation, precipitation, adsorption, membrane separation, etc. Thus, advanced oxidation processes (AOP's) become one of the superior methods used and widely studied for the degradation these organic pollutants. Heterogeneous photocatalysis using nano-TiO<sub>2</sub> as the photocatalyst was studied in this project. Nano-TiO<sub>2</sub> was successfully prepared using acid-catalyzed sol-gel method and the as-synthesized photocatalyst was characterized using Brunauer-Emmett-Teller (BET), X-ray diffraction (XRD), transmission electron microscopy (TEM) and UV-Vis diffuse reflectance spectroscopy (UV-Vis DRS). Photocatalytic activity of the prepared TiO<sub>2</sub> was tested by the photodegradation of phenol solution in a batch reactor. Hydroxypropyl cellulose (HPC) was added into the TiO<sub>2</sub> during the sol preparation as surfactant. Addition of 1g/L of HPC into the TiO<sub>2</sub> was found to successfully reduce the particles agglomeration and resulted in TiO<sub>2</sub> with higher surface area which showed better photocatalytic activity in comparison to TiO<sub>2</sub> without surfactant and commercial available TiO<sub>2</sub> Degussa P-25. Effect of metal doping was studied by doping TiO<sub>2</sub> with Fe<sup>3+</sup>. 0.25 wt% of Fe<sup>3+</sup> was found to be the optimum dopant concentration. Response surface methodology (RSM) based on Box-Behnken design (BBD) was

used to evaluate the effects of operating parameters. Photocatalyst concentration = 0.94g/L, phenol concentration = 10.48mg/L and  $\text{Fe}^{3+}$  concentration = 0.25 wt% are the optimum conditions for photodegradation of phenol. The prepared photocatalyst successfully decomposed 98.24% and 85.0% of phenol in near UV ( $\lambda = 365\text{nm}$ ) and direct solar light illumination, respectively.

# **CHAPTER 1**

## **INTRODUCTION**

This chapter covers the overview of water contaminations, problem statement, scope as well as objectives of the study, then, followed by the organization of the thesis.

### **1.1 OVERVIEW OF WATER CONTAMINATIONS**

The world's most precious and important natural resource, water, is under threat from various contaminants, causing a water contamination crisis. While the world's population has been tripled in the 20<sup>th</sup> century, use of renewable water resources has grown six-fold, and global population is expected to increase by another 40% to 50% within the next 50 years. The increasing demand for water generated by this population growth will cause serious consequences on the environment (Water Crisis, 2009). According to the World Health Organization (WHO), in 2002 more than one out of six people lacked access to safe drinking water, namely 1.1 billion people, representing 17% of the global population. Moreover, in the same year, 2.6 billion people i.e. 42% of the world's populations were without even the most basic sanitation facilities. A lack of clean drinking water and sanitation facility kills about 4,500 children each day and condemns their parents, siblings, and neighbors to sickness, pollution, and enduring poverty (Water, sanitation and hygiene links to health, 2009). It should be noted that these figures represent only those people living in very poor conditions. In reality, the overall figures are expected to be much higher (Teh and Mohamed, 2011).

Humans are generating and disposing more wastewater today than any other time. The disposal of toxic contaminants, such as dyes and phenolic compounds which are harmful to the environment, hazardous to humans, and difficult to degrade by natural means, is pervasively associated with industrial development and these contaminants are frequently found in the industrial effluents (Fernández *et al.*, 2010). Chemical precipitation, filtration, electro-deposition, ion-exchange adsorption, and membrane systems are some of the conventional methods for water treatment and have found certain practical applications. However, these methods may not be very effective, because they are either slow or nondestructive to some or more persistent organic pollutants. Besides, large scale implementations of these methods have some limitations, owing to the expensive equipments involved in the processes (Panda *et al.*, 2010). It is therefore essential to investigate the use of efficient catalytic materials to remove highly toxic compounds from potential sources of drinking water by using a more cost saving and efficient method.

Semiconductor heterogeneous photocatalysis is a popular technique that has the great potential to control the organic contaminants in water or air (Shu *et al.*, 2010). This process which is also known as Advanced Oxidation Process (AOP) is suitable for the oxidation of recalcitrant contaminants such as dyes and phenolic compounds (Rossetto *et al.*, 2010). Heterogeneous photocatalytic oxidation, developed in the 1970s, has attracted considerable attention particularly when used under solar light (Yurdakal *et al.*, 2008). In the past decades, numerous studies have been carried out by researchers from all over the world on the application of heterogeneous photocatalytic oxidation process to decompose and mineralize certain recalcitrant contaminants. The photocatalytic activity of various forms of TiO<sub>2</sub>, such as TiO<sub>2</sub> film (Zhang *et al.*, 2010b), TiO<sub>2</sub> powders (Tian *et al.*, 2009b), TiO<sub>2</sub>

nanotubes (Sreekantan and Wei, 2010), supported TiO<sub>2</sub> (Toni *et al.*, 2010, Khataee *et al.*, 2010, Velasco *et al.*, 2010) and doped TiO<sub>2</sub> (Naeem and Ouyang, 2010, Yu and Yang, 2010) have been evaluated through degradation of dyes and/or phenolic compounds under light irradiation. Results of these studies show that TiO<sub>2</sub> is effective for removing dyes and phenolic compounds from aqueous solutions.

## 1.2 PROBLEM STATEMENT

The world's most precious and important natural resource, i.e. water is being threatened by various contaminants, causing a water contamination crisis. Phenol has been detected in industrial wastewater and been characterized as a carcinogenic compound that would pose fatal effects to human and other living creatures that have exposed to it. The level of phenols in Linggi River, Negeri Sembilan, Malaysia was found to exceed the recommended Malaysian standard of 2.0 µg/L for raw water (Sarmani *et al.*, 1992). This is seen as the direct impact of industrial and urbanization of the area. Excess exposure to phenols may cause central nervous system impairment and liver and kidney damage (Occupational Safety and Health Guideline for Phenol, 2011). Therefore, a discharge limit of phenols in inland water, i.e. 0.001ppm for Standard A and 1ppm for Standard B has been set under the environmental quality (sewage and industrial effluents) regulations, 1979 by the Department of Environment (DOE).

Titanium dioxide (TiO<sub>2</sub>) nanoparticles have been proven to be an important and effective photocatalyst for the degradation of environmental contaminants (Dimitrijevic *et al.*, 2005). Nonetheless, there are still plenty of problems need to be solved for practical application of TiO<sub>2</sub> nanoparticles for photocatalysis. Agglomeration of nano-sized TiO<sub>2</sub> particles into bigger sized particles always occur

and this will reduce the porosity and specific surface area of the catalyst which eventually decrease the efficiency of its photocatalytic activity. Besides, photogenerated electron/hole pairs have higher tendency for recombination when pure TiO<sub>2</sub> is used as photocatalyst and this will reduce the efficiency of photocatalytic degradation of phenol.

Furthermore, pure TiO<sub>2</sub> has relatively large band gap energy (3.2eV) and this makes it only applicable under the illumination of UV radiation with short wavelength of about 256nm. Moreover, bigger band gap energy means higher input energy is required for the electronic excitation of TiO<sub>2</sub> nanoparticles. As a result, the photonic efficiency of the pure TiO<sub>2</sub> is less than 10% for most of the photocatalytic decomposition processes and its application as a photocatalyst with solar light is very much limited (Peng and Peng, 2000, Jun *et al.*, 2002, Cozzoli *et al.*, 2003). Thus, it is highly sought-after to synthesize TiO<sub>2</sub> nanoparticles with a high photocatalytic activity. One way to enhance the photocatalytic performance of TiO<sub>2</sub> is by manipulating the physical properties of the semiconductor such as shape, size and surface properties. Besides, energy band gap of the photocatalyst also has to be reduced by adding suitable amounts of dopants (Liao *et al.*, 2008). The coupling effects of hydroxypropyl cellulose (HPC) as surfactant and Fe<sup>3+</sup> as dopant on photocatalytic activity of TiO<sub>2</sub> will be studied in this project.

### **1.3 RESEARCH OBJECTIVES**

The overall objective of this study is to develop metal-doped TiO<sub>2</sub> photocatalyst by sol-gel method for the removal of phenol in aqueous solutions. The objectives of the study are to:

- Synthesize and characterize the physical and chemical properties of Fe-doped TiO<sub>2</sub> based catalyst
- Study the effects of surfactant on inhibiting the nano-sized TiO<sub>2</sub> agglomeration
- Study the performance of the developed photocatalyst for the photocatalytic degradation of phenol in the batch reactor under a wide range of process and compare with commercial catalyst
- Study the kinetic of photocatalytic degradation of phenol in the batch reactor
- Study the effects of dopants on the photocatalytic activity of TiO<sub>2</sub> under UV (365nm) and direct solar irradiation.

### **1.4 SCOPE OF STUDY**

This study emphasizes on the synthesis of highly efficient nano TiO<sub>2</sub> using acid catalyzed sol-gel method. The effects of surfactant and dopant addition into the photocatalyst are studied. Hydroxypropyl cellulose (HPC) with concentration varied from 0-1g/L is used as the surfactant. HPC was chosen in this study because it is soluble in both water and polar organic solvents, has no medical effect, nor toxicity as well as stable even under lightly acidic or alkaline conditions. While iron(III) nitrate nonahydrate (Fe(NO<sub>3</sub>)<sub>3</sub>.9H<sub>2</sub>O) is chosen as the metal dopant. The prepared photocatalysts are characterized using transmission electron microscopy (TEM), X-



ray diffraction (XRD), Brunauer-Emmett-Teller (BET) surface area and UV/Vis – diffuse reflectance spectroscopy (UV/Vis DRS). While the photocatalytic activity of the prepared photocatalysts, is tested by photodegradation of phenol in batch reactor.

Several operating parameters which include catalyst loading (0.1g/L-1.5g/L), pH (3-10), initial phenol concentration (10-90mg/L) and dopant ( $\text{Fe}^{3+}$ ) concentration (0.00 – 0.75wt%) are studied to determine the performance of the prepared  $\text{TiO}_2$ . The range of operating parameters studied in this project were chosen based on studies by Chiou et al. (2008a), Muruganandhan and Swaminathan (2006) as well as Bayarri et al. (2005).  $2^3$  factorial experimental design of response surface methodology (RSM) is used to study the possible interaction between the process parameters on phenol degradation. RSM is also used as a tool to determine the optimum condition for phenol degradation in a batch reactor. Last but not least, the reaction rate of phenol degradation is studied based on Langmuir-Hinshelwood kinetics model.

## **1.5 ORGANIZATION OF THESIS**

This thesis consists of five different chapters. In Chapter 1, the introduction briefly discuss the current situation of water contamination particularly by industrial effluents and the effects of water contamination on living creatures as well as the possible ways of solving this problem. Problem statement that describes the problem faced and the necessary of this research is also being discussed in this chapter. Following problem statement are the scope and objectives of study which discuss what are being studied and the purposes of this research respectively. This is then followed by the organization of the thesis.

Literature review is the second chapter of this thesis. In this chapter, a detailed search of published reports on the advancement in photocataysis field has

been carried out and analyzed. It includes discussion on the target pollutants of this project, i.e. phenolic compounds, decomposition of organic pollutants in wastewater by photocatalytic reactions, introduction of the semiconductor photocatalyst (titanium dioxide), additive materials to photocatalyst such as surfactant and dopants, and lastly design of experiment.

Chapter 3, materials and method presents the experimental part of the research. In the first part of this chapter, details of the materials and chemical reagents as well as a general description about the photocatalytic reactor used in the research have been presented. The following part covers the detailed description of the photocatalyst preparation steps and characterization methods. Finally, it is followed by the discussion on process studies and experimental design of this research.

Chapter 4, results and discussion provides the experimental findings, results and their discussion. It is divided into four parts which include effects of surfactant, kinetic studies, effects of dopant and mineralization studies of phenol using synthesized photocatalyst.

Last but not least, conclusions and recommendations are included in chapter 5. This part summarizes the results and findings reported in chapter 4. Recommendations on the possible ways to improve the present study are also discussed in this chapter.

## CHAPTER 2

### LITERATURE REVIEW

This chapter covers the background information on heterogeneous photocatalysis process. It includes discussion on the target pollutants of this project, i.e. phenolic compounds, decomposition of organic pollutants in wastewater by photocatalytic reactions, introduction of semiconductor photocatalyst (titanium dioxide), additive materials to photocatalyst such as surfactant and dopants, and lastly design of experiment.

#### 2.1 PHENOLIC COMPOUNDS

The presence of phenols and their derivatives in water supplies and industrial effluents is a problem that attracts global concern. These hazardous water-soluble phenolic compounds are continuously released to the environment through domestic and industrial activities, representing a severe toxicological risk to the earth as well as all living creatures on it.

Phenolic compounds are aromatic compounds with one or more hydroxyl groups attached to the aromatic ring. These compounds are usually found in wastewater discharged from a variety of industries, such as chemical synthesis, plastics, coke plants, resin manufacturing, petrochemical, oil-refineries, iron smelting, dyes, pulp and paper, textiles, detergents, pharmaceuticals, as well as pesticides and herbicides synthesis (Li *et al.*, 2005, Wang *et al.*, 2005, Adán *et al.*, 2007, Yang *et al.*, 2009a). Phenolic derivatives also have widespread applications in the synthesis of plastics, colors, pesticides and insecticides, where they are used as intermediates (Saravanan *et al.*, 2009). Besides, phenolic compounds can also arise from natural

sources in the aquatic environment, such as algal secretion, lignin transformation, hydrolysable tannins and flavanoids, and humidification processes at low concentration (Zainudin *et al.*, 2009).

Humans are potentially exposed to phenol and its derivatives in all places, as they are found in tea, fruits, and vegetables and are widely used in industrial processes, pharmaceuticals, and consumer products (Hansch *et al.*, 2000). Exposure to phenols poses hazards to humans as the compounds are corrosive to the respiratory tract, eyes, and skin. Repeated or long-term exposure of skin to phenols will cause dermatitis, or even second- and third-degree burns because of the phenol's defatting and caustic properties (Lin *et al.*, 2006, M.J. O'Neil *et al.*, 2006). Therefore, a discharge limit of phenols in inland water, i.e. 1mg/L has been set under the environmental quality (sewage and industrial effluents) regulations, 1979 by the Department of Environment (DOE) (Parameter Limits of Effluents under Environmental Quality (Sewage & Industrial Effluents) Regulations 1979, 2008).

Phenol derivatives such as bisphenol A (BPA), chlorophenol, and nitrophenol are also known to be hazardous to humans. BPA is an organic compound with two phenol functional groups, which is widely used in the plastics industry for the production of polycarbonate plastics and epoxy resins. Dental composites/sealants, baby bottles, the lining of food cans, and drinking-water bottles are some of the consumer products developed from BPA. The presence of BPA in industrial effluents has received wider attention since it was listed as an endocrine-disrupting chemical (EDC), which can influence the generative function of humans and other living creatures by mimicking the body's own hormones and leads to negative health effects (Nakashima *et al.*, 2002, Tsai, 2006).

The next phenol derivative, chlorophenol, is an organochloride of phenol, usually consisting of one or more covalently bonded chlorine atoms. It is also a known endocrine disruptor that is toxic and non-biodegradable. This compound is an important xenobiotic micropollutant of aquatic environments and is usually present in wastewater as by-products of the pulp and paper, dyestuff and pharmaceutical industries (Theurich *et al.*, 1996, Venkatachalam *et al.*, 2007). Besides, chlorophenol is extensively used as intermediate in the production of insecticides, herbicides, preservatives, antiseptics, disinfectants and other organic compounds (Gu *et al.*, 2010). Biodegradation of chlorophenol is slow and incomplete, eventually generating by-products that are more toxic and hazardous than chlorophenol to the environment as well as to human health (Sherrard *et al.*, 1996, Jain *et al.*, 2004).

Whereas for nitrophenols, it is another family of common phenolic compounds found in industrial effluents, are continually detected in urban and agricultural waste as they are among the most widely used and versatile industrial organic compounds. These compounds are usually used in the manufacture of pharmaceuticals, pesticides, explosives, dye, pigments, wood preservatives, and rubber chemicals. Nitrophenols have been proven to be carcinogenic and may pose significant health risks to humans and other organisms. Among the nitrophenols, 2-nitrophenol, 4-nitrophenol, and 2, 4-dinitrophenol have been listed as “Priority Pollutants” by the US Environmental Protection Agency, which recommended that their concentrations in natural waters should be restricted to below 10 ng/l (Weihua *et al.*, 2002, Gemini *et al.*, 2005, She *et al.*, 2005, Sponza and Kuşçu, 2005, Wang *et al.*, 2009).

In short, phenol and its derivatives are refractory and toxic pollutants in the natural environment. Moreover, the time needed for these compounds to degrade and

disappear chemically in air is not known. They are able to partially biodegrade in water and surface soil. However, this depends on conditions whereby they take longer time to degrade at lower soil depths and groundwater. Hence, phenol and its derivatives are expected to stay longer in the deep soil of dump sites in comparison to surface soil and sometimes may even stay indefinitely in these soils (Shukla *et al.*, 2009). Therefore, there is a pressing need to develop effective method for the treatment of these pollutants which is of low cost and less time consuming, so as to turning them into less harmful compounds or to their complete mineralization.

## **2.2 DECOMPOSITION OF ORGANIC POLLUTANTS IN WASTEWATER BY PHOTOCATALYTIC REACTIONS**

From the perspective of environmental science, regulatory laws, and human health, it is urgent that the release of toxic chemicals from industrial processes must be restricted. In fact, many processes and technologies for destroying these toxics have been proposed over the years, and some are currently employed in a number of wastewater treatment plants. Among the various methods used for the decomposition of these toxic compounds, a more promising technology based on an advanced oxidation process has been extensively studied. This process involves the degradation of pollutants by irradiating suspensions of metal oxide semiconductor particles such as TiO<sub>2</sub> or zinc oxide (ZnO) with light. It is a promising method because it not only degrades the pollutants but also completely mineralizes them to carbon dioxide (CO<sub>2</sub>), water (H<sub>2</sub>O), and mineral acids (Lachheb *et al.*, 2002, Karkmaz *et al.*, 2004, Gupta *et al.*, 2006). The low-cost and mild operating conditions (mild temperature and pressure) of this photocatalytic degradation process are also factors in its popularity in wastewater treatment (Bhatkhande *et al.*, 2002).

### 2.3 SEMICONDUCTOR PHOTOCATALYST: TITANIUM DIOXIDE (TiO<sub>2</sub>)

A semiconductor is a material with electrical resistivity between that of an insulator and a conductor and is usually characterized by an electronic band structure in which the lowest empty energy bands, called the conduction band (CB), and the highest occupied energy band, called the valence band (VB), are separated by a band gap. The ability of a photocatalytic reaction to degrade organic and inorganic pollutants arises from the redox environment generated from the photoactivation of a semiconductor such as titanium dioxide (TiO<sub>2</sub>). In general, three components must be present so that the heterogeneous photocatalytic reaction can occur: an emitted photon (in the appropriate wavelength), a strong oxidizing agent (usually oxygen), and a catalyst surface (a semiconductor material) (Kaneko and Okura, 2002).

Titanium dioxide (TiO<sub>2</sub>) is a natural occurring oxide of titanium. It is also named as titania or titanium(IV) oxide. In nature, TiO<sub>2</sub> exists in five different forms, i.e. rutile, anatase, brookite, monoclinic and orthorhombic. However, monoclinic and orthorhombic phase of TiO<sub>2</sub> are two exceptions found only in shocked granet gneisses from Ries crater in Germany (Goresy *et al.*, 2000, Goresy *et al.*, 2001). Rutile appears to be the most common form of TiO<sub>2</sub>, while anatase and brookite forms of TiO<sub>2</sub> tend to convert into rutile form upon heating at high temperature. Calcinated TiO<sub>2</sub>, especially in rutile form is very stable and insoluble in water; it is also insoluble or only moderately soluble in concentrated and hot acids (Wrinkler, 2003).

TiO<sub>2</sub> is well known for its widespread applications in paints, sunscreens, environmental treatment and purification purposes (Auvinen and Wirtanen, 2008, Carlotti *et al.*, 2009, Liao and Que, 2010, Mohamed and Mkhaliid, 2010). These are

credited to its high level of photoconductivity, ready availability, low toxicity, inertness, low cost as well as high photoefficiency and activity. Crystalline structure of TiO<sub>2</sub> has been reported as one of the factors affecting its photocatalytic activity. Anatase form of TiO<sub>2</sub> has the best photocatalytic activity, followed by rutile form (Ray *et al.*, 2009).

TiO<sub>2</sub> can utilize natural UV radiation from sunlight for photocatalysis because it has suitable energetic separation between its conduction and valence band (Saravanan *et al.*, 2009). Band gap energy of TiO<sub>2</sub> (3.2eV for anatase; 3.03 for rutile) is relatively smaller compared to other semiconductors, such as ZnO (3.35eV) and SnO<sub>2</sub> (3.6eV) (Schiavello, 1997). Therefore, TiO<sub>2</sub> is able to absorb photons energy in the near UV range ( $\lambda < 387\text{nm}$ ). The positions of band edges of some semiconductors are shown in Figure 2.1 using the normal hydrogen electrode (NHE) scale as reference. The energy level at the bottom of conduction band corresponds to the reduction potential of the photogenerated electrons. Whereas, the oxidizing ability of the photogenerated holes is represented by the energy level at the top of valence band. Each value at the top and bottom shows the ability of the corresponding system to promote oxidation and reduction reactions. All semiconductors could be photocatalysts but only certain shows photocatalytic properties (Carp *et al.*, 2004).

Photocatalytic reaction is initiated with the sufficient input of radiation equal or higher than the band-gap energy of the target semiconductor which causes molecular excitation and charge separation. As a result, mobile electrons and holes will be generated and migrate to the surface of the semiconductor to take part in the photocatalytic reaction (Chun *et al.*, 2000). Mechanism of the photocatalytic reaction will be further discussed in later part of this article.



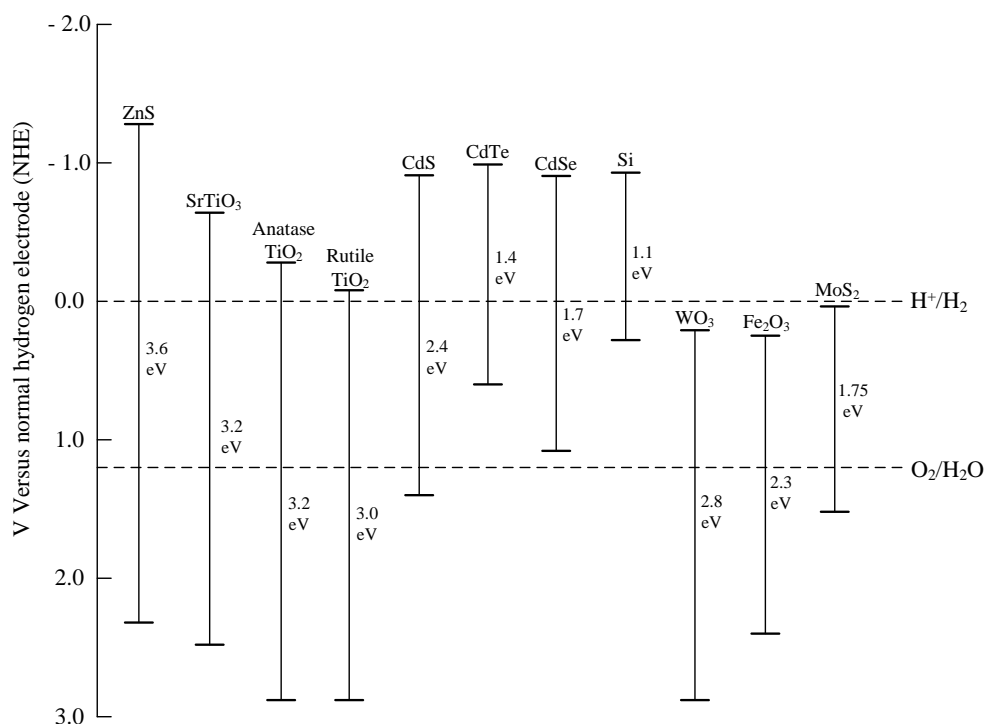


**Figure 2.1:** Positions of band edges of some semiconductors in contact with aqueous electrolyte (Schiavello, 1997).

## 2.4 MECHANISM OF PHOTOCATALYTIC REACTION

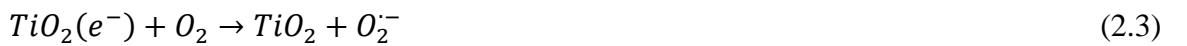
The heterogeneous photocatalytic reaction is initiated with the absorption of radiation equal to or higher than the band gap energy ( $E_{bg}$ ) of the target semiconductor.  $E_{bg}$  is defined as the difference between the filled VB and the empty CB; in this case  $TiO_2$  has a band gap of 3.2 eV in the form of anatase or 3.0 eV as rutile. When photons with energy equal to or higher than  $E_{bg}$  reach the surface of the photocatalyst, they will cause molecular excitation. As a result, mobile electrons will be generated in the higher-energy CB simultaneously with the generation of positive holes in the lower-energy VB of the photocatalyst.



After the initiation of photogenerated electron–hole pairs, the photocatalytic reaction will proceed through a series of chemical events. The photogenerated holes and electrons can either recombine and dissipate the absorbed energy as heat or be available for use in the redox reaction. Photogenerated holes and electrons that do not recombine migrate to the surface of catalyst for redox reaction. The redox reaction will utilize both the electrons and holes, with the positive holes ( $h^+$ ) for oxidation processes and the electrons ( $e^-$ ) for reduction processes on the surface of the photocatalysts. The positive holes break apart the water molecule to form hydron (positive hydrogen cation,  $H^+$ ) and the hydroxide ion ( $OH^-$ ) as shown in equation 2.2. This  $OH^-$  will then lead to the production of strong oxidizing  $HO^\bullet$  radicals.



Meanwhile, the negative electrons react with the oxygen molecule to form a superoxide anion ( $O_2^{\bullet -}$ ).



This superoxide anion also produces  $HO^\bullet$  radicals via the formation of  $HO_2^{\bullet}$  radicals and  $H_2O_2$ . Equations (2.4) – (2.6) show the reactions of superoxide anions,  $O_2^{\bullet -}$  to form  $HO_2^{\bullet}$  radicals and  $H_2O_2$ . Photoconversion of the resulted hydrogen peroxide ( $H_2O_2$ ) will give more  $HO^\bullet$  free-radicals groups as shown in equation (2.7).





The electron–hole recombination step is undesirable as it will result in process inefficiencies and waste the energy supplied by the photon. Therefore, it is often considered as one of the major factors limiting the efficiency of the photocatalytic processes. Besides, it is found that  $HO \cdot$  is the most plentiful radical species in  $TiO_2$  aqueous suspension and the reaction of  $HO \cdot$  with organic pollutants is the most important step that leads to the mineralization of organic pollutants (Lasa *et al.*, 2005, Puma *et al.*, 2008, Saravanan *et al.*, 2009).

In short, the heterogeneous photocatalytic reaction can basically be represented by six mechanistic steps ( Kaneko and Okura, 2002):

1. Absorption of one unit of light associated with the formation of a conduction band electron and a valence band hole in the semiconductor.
2. Transfer of the generated electron ( $e^-$ ) and hole ( $h^+$ ) to the surface.
3. Recombination of electron-hole pairs during the reaction processes.
4. Stabilization of a hole and an electron at the surface of the semiconductor to form a trapped hole and a trapped electron respectively.
5. Reduction and oxidation of molecules occur on the surface of the semiconductor.
6. Exchange of product at the surface with a reactant at a medium.

The absorption of light in the bulk (Step 1) and the subsequent redox reactions at the surface (Step 5) are the key processes in photocatalysis out of these six reaction steps. Step 2 and/or Step 4 sometimes occur too fast to be included in the steps. Transfer of generated electron and hole to the surface (Step 2) and reduction/oxidation of

molecules at the surface (Step 5) are affected by crystallite size of the semiconductor, where these paths will increase with decreasing particle size (Kaneko and Okura, 2002). Figure 2.2 shows the processes of photocatalysis at a semiconductor particle.

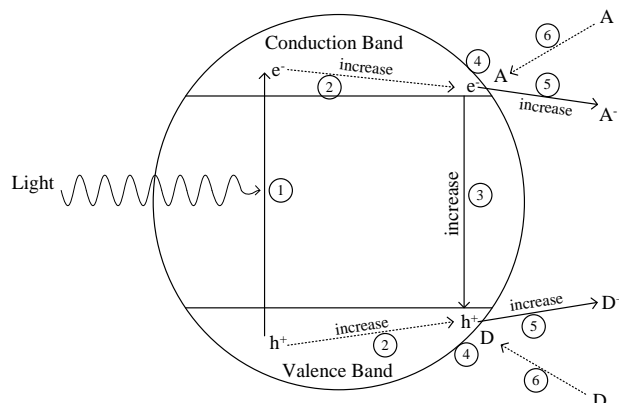


**Figure 2.2:** Processes of photocatalysis at semiconductor particles. The numbers represent to the mechanistic steps in the text. Paths 2 and 5 which increase with decreasing crystallite size of the particle are shown by “increase” (Kaneko and Okura, 2002).

The process of phenol degradation is initiated by the generated  $HO^{\bullet}$  radicals and proceeds with a series of intermediary steps before mineralized into water ( $H_2O$ ) and carbon dioxide ( $CO_2$ ) (Okamoto *et al.*, 1985, Matos *et al.*, 1998, Matos *et al.*, 2007, Silva and Faria, 2009a). Single substituted hydroxyl derivatives such as catechol (CT: 2-hydroxyphenol) and hydroquinone (HQ: 4-hydroxyphenol) are detected as the main intermediates. Traces of resorcinol, pyrogallol (PG) and benzoquinone (BQ) are also detected (Silva and Faria, 2009a). Then, the phenyl rings of these intermediary compounds will be broken up to give ring opening products such as acetic, formic, maleic and oxalic acids. Further oxidation of these short chain organic acids will finally yield the desired end products, which are  $H_2O$  and  $CO_2$

(Silva and Faria, 2009a). A simplified reaction mechanism of phenol degradation is shown in Figure 2.3 (Okamoto *et al.*, 1985).

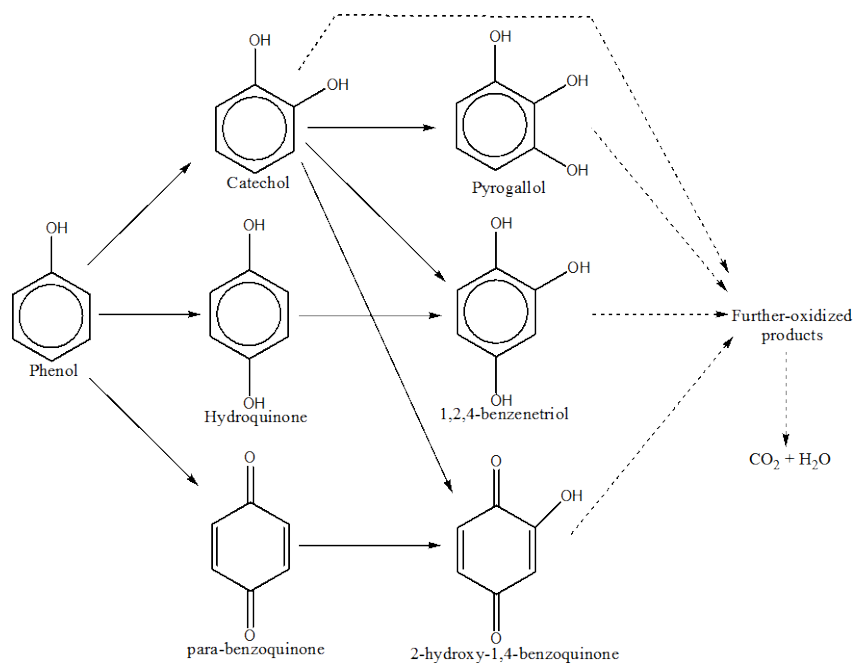


**Figure 2.3:** Simplified reaction mechanism of phenol degradation (Okamoto *et al.*, 1985).

## 2.5 PHOTOCATALYTIC DEGRADATION OF PHENOLIC COMPOUNDS USING TiO<sub>2</sub>

Over the years, the feasibility and efficiency of the photodecomposition of phenol and its derivatives in water using TiO<sub>2</sub> as photocatalyst have attracted the attention of researchers. Thus, many studies have been carried out to examine the photocatalytic degradation of these pollutants in the presence of photocatalyst. The efficiency and rate of the photodegradation of phenol and its derivatives were found to be dependent on light intensity, catalyst concentration, solution pH, substrate (phenol and its derivatives) concentration, physical properties of the catalyst and the presence of electron acceptor.

Studies by of Zainudin *et al.* (2009) and Xiao *et al.* (2008) proved that photocatalytic performance of TiO<sub>2</sub> can be improved by enlarging the catalysts surface area. They also showed that high crystalline quality of the synthesized catalyst was able to reduce the rate of electron-hole pair recombination. Photocatalytic efficiency was found to be somehow dependent on light intensity. Hosseini *et al.* (2007) proved that the efficiency of photocatalysis increased about twice when they increased the UV intensity from 80W to 125W. Kaneco *et al.* (2004) and Shukla *et al.* (2009) also showed that higher light intensity gives better results in decomposing the target pollutants.

The effects of solution pH, catalyst concentration and substrate (phenol and its derivatives) concentration were studied by Zainudin *et al.* (2009), Silva and Faria (2009a), Kaneco *et al.* (2004), Chiang *et al.* (2004), Tsai *et al.* (2009), Wang *et al.* (2009), Shukla *et al.* (2009) and Gu *et al.* (2010). In general, the degree of mineralization was relatively lower at solution pH higher than 7. This is because

TiO<sub>2</sub> particle surface becomes negatively charged at alkaline conditions and will inhibit the adsorption of substrate onto its surface, which eventually lowers the ability of pollutants mineralization by the catalyst. There exists an optimum amount of catalyst loading and substrate concentration, whereby the degree of photodegradation becomes lower when the concentration of catalyst and/or substrate concentration are lower or higher than this optimum value.

The results of these studies are summarized in Table 2.1.

**Table 2.1:** Summary of studies on photocatalytic degradation of phenolic compounds in wastewater in the presence of TiO<sub>2</sub> as photocatalyst

Compound degraded	Photocatalyst used	Parameter studied	Comments	References
Phenol	Nanocrystalline TiO <sub>2</sub> prepared by acid-catalyzed sol-gel method	Catalyst loading, initial phenol concentration, pH, irradiation intensity, and presence of oxidant species	<ul style="list-style-type: none"><li>• Photocatalytic process was influenced by operating parameters.</li><li>• Introduction of oxidant moderately increased the oxidation rate, but the increase did not depend on the nature of the oxidant. This suggests that the oxidant process is mainly due to the HO• adsorbed radicals generated from positive holes at the surface.</li></ul>	(Silva and Faria, 2009a)
Phenol	Supported nano-TiO <sub>2</sub> /ZSM-5/silica gel (SNTZS)	TiO <sub>2</sub> loading, adsorbent (zeolite) loading, support loading, and binder (colloidal silica gel) loading	<ul style="list-style-type: none"><li>• Optimum formulation of SNTZS = nano-TiO<sub>2</sub>: ZSM-5:silica gel:colloidal silica gel = 1:0.6:0.6:1.</li><li>• High photocatalytic activity of SNTZS was due to its large surface area (275.7 m<sup>2</sup>/g), high crystalline quality of the synthesized catalyst, small particle size, and low electron-hole pair recombination rate.</li></ul>	(Zainudin <i>et al.</i> , 2009)
Phenol	Nano-sized TiO <sub>2</sub> prepared by hydrogen-air flame hydrolysis	Effect of particle shape on the activity of nanocrystalline TiO <sub>2</sub>	<ul style="list-style-type: none"><li>• Particle shape played a crucial role in the photocatalytic activity, where samples with only polyhedral (faceted) nanocrystals significantly showed better photocatalytic degradation of phenol compared to those containing a mixture of spherical and polyhedral nanocrystals.</li></ul>	(Balázs <i>et al.</i> , 2008)



**Table 2.1:** (Continued)

<b>Compound degraded</b>	<b>Photocatalyst used</b>	<b>Parameter studied</b>	<b>Comments</b>	<b>References</b>
Phenol	TiO <sub>2</sub> Degussa P-25	Effect of adding hydrogen peroxide (H <sub>2</sub> O <sub>2</sub> )	<ul style="list-style-type: none"><li>• The combined use of TiO<sub>2</sub> photocatalyst, H<sub>2</sub>O<sub>2</sub>, and UV light greatly improved the efficiency of phenol degradation. This could be explained by the ability of H<sub>2</sub>O<sub>2</sub> to produce hydroxyl radicals under UV irradiation, thereby increasing photodegradation.</li></ul>	(Chiou <i>et al.</i> , 2008a)
Phenol	TiO <sub>2</sub>	Influence of calcinations temperature (350°C-750°C)	<ul style="list-style-type: none"><li>• Lower calcinations temperature (350 °C) led to highest photocatalytic activity in visible light (<math>\lambda &gt; 400</math> nm). This is because lower calcinations temperature favors a larger surface area, more residual carbon in the form of carbonaceous C-C species (working as sensitizers), elimination of oxygen vacancies, and promotion of photocatalytic activity under visible light.</li><li>• Increasing calcinations temperature to 450°C diminishes the amount of carbonaceous species and suppresses the activity under visible light. However, TiO<sub>2</sub> calcined at this temperature had the best activity in UV light (<math>250 &lt; \lambda &lt; 400</math> nm).</li></ul>	(Górska <i>et al.</i> , 2008)

**Table 2.1:** (Continued)

<b>Compound degraded</b>	<b>Photocatalyst used</b>	<b>Parameter studied</b>	<b>Comments</b>	<b>References</b>
Phenol	Nanocrystalline anatase TiO <sub>2</sub> prepared by sol-gel method	Size effects of TiO <sub>2</sub>	<ul style="list-style-type: none"><li>• When the TiO<sub>2</sub> crystal size decreased from 9.9 to 4.5 nm, the semiconductor bandgap shifted toward a higher energy level.</li><li>• The optimal TiO<sub>2</sub> particle size (about 10 nm) for maximum photocatalytic efficiency is claimed to be a result of photogenerated electrons and holes, light absorption, defects, and surface area.</li></ul>	(Liu <i>et al.</i> , 2008)
Phenol	TiO <sub>2</sub> loaded on mesoporous graphitic carbon (TiO <sub>2</sub> /GC-950)	N/A	<ul style="list-style-type: none"><li>• TiO<sub>2</sub>/GC-950 showed better photoactivity than pure TiO<sub>2</sub> with reaction constant, <math>k_1</math> of 0.012min<sup>-1</sup> (0.008min<sup>-1</sup> for pure TiO<sub>2</sub>).</li><li>• This enhancement in photoactivity was due to the confinement in the mesopores of graphitic carbon (GC-950), which improved the adsorption ability of phenol molecules by providing larger surface area.</li><li>• Besides, high degree of anatase crystallization with less defect sites which could reduce recombination of electrons/holes as well as the graphitic property of GC-950 that facilitated the diffusion of reactants and products from the active site also led to the improvement in photocatalytic activity.</li></ul>	(Xiao <i>et al.</i> , 2008)

**Table 2.1:** (Continued)

<b>Compound degraded</b>	<b>Photocatalyst used</b>	<b>Parameter studied</b>	<b>Comments</b>	<b>References</b>
Phenol	TiO <sub>2</sub> coated on perlite	Effect of light intensity	<ul style="list-style-type: none"> <li>• High porosity of perlite (&gt;95%) allowed TiO<sub>2</sub> coated on it to float on water surface and thus no filtration and recirculation were needed to get back the catalyst after the reaction.</li> <li>• Photocatalytic efficiency increased about twice with the increase of UV intensity from 80W lamp to 125W lamp.</li> </ul>	(Hosseini <i>et al.</i> , 2007)
Phenol	Pellet and powder forms of TiO <sub>2</sub> deposited on activated carbon (AC)	N/A	<ul style="list-style-type: none"> <li>• Both TiO<sub>2</sub>/AC pellet and TiO<sub>2</sub>/AC powder showed good performance in photodegradation of phenol in aqueous solution.</li> </ul>	(Carpio <i>et al.</i> , 2005)
Bisphenol A (BPA)	Nano-TiO <sub>2</sub> purchased from Degussa AG Co.	Initial BPA concentration, photocatalyst dosage, initial pH, temperature	<ul style="list-style-type: none"> <li>• Optimal conditions for photocatalytic degradation of BPA could be performed at initial BPA concentration = 20 mg/L, TiO<sub>2</sub> dosage = 0.5 g/L (100 mg / 200 cm<sup>3</sup>), initial pH = 7.0, and temperature = 25°C.</li> <li>• Photodegradation kinetics for the destruction/removal of BPA in water can be well described by a pseudo-first-order reaction model, where the apparent first-order reaction constant (<math>k_{obs}</math>) is proportional to TiO<sub>2</sub> dosage.</li> </ul>	(Tsai <i>et al.</i> , 2009)